

Fermi National Accelerator Laboratory

FERMILAB-Pub-83/27-EXP

7420.616

Phys. Rev. Lett. 51, 343 (1983)

MEASUREMENT OF THE RATE OF INCREASE OF NEUTRINO CROSS SECTIONS WITH ENERGY

R. Blair, B. Barish, Y. K. Chu, B. Jin,
D. MacFarlane, R. L. Messner, J. Lee, J. Ludwig,
D. B. Novikoff and M. V. Purohit
California Institute of Technology, Pasadena, California 91125

P. S. Auchincloss, F. Sciulli, and M. H. Shaevitz
Columbia University, New York, New York 10027

F. Bartlett, D. Edwards, H. Edwards, H. E. Fisk, Y. Fukushima,
Q. A. Kerns, T. Kondo, P. A. Rapidis, S. L. Segler,
R. J. Stefanski, D. Theriot, and D. Yovanovitch
Fermi National Accelerator Laboratory, Batavia, Illinois 60510

A. Bodek, R. Coleman, and W. Marsh
University of Rochester, Rochester, New York 14627

and

O. Fackler and K. A. Jenkins
Rockefeller University, New York, New York 10021

October 1983

Measurement of the Rate of Increase of Neutrino
Cross Sections with Energy

R. Blair,^a B. Barish, Y.K. Chu, B. Jin,^b
D. MacFarlane, R.L. Messner,^c J. Lee,^d J. Ludwig,^e
D.B. Novikoff,^f M.V. Purohit

California Institute of Technology, Pasadena, CA 91125

P.S. Auchincloss, F. Sciulli, M.H. Shaevitz

Columbia University, New York, NY 10027

F. Bartlett, D. Edwards, H. Edwards, H.E. Fisk,
Y. Fukushima,^g Q.A. Kerns, T. Kondo,^g P.A. Rapidis,
S.L. Segler, R.J. Stefanski, D. Theriot, D. Yovanovitch

Fermi National Accelerator Laboratory, Batavia, IL 60510

A. Bodek, R. Coleman,^h W. Marsh^h

University of Rochester, Rochester, NY 14627

O. Fackler, K.A. Jenkins

Rockefeller University, New York, NY 10021

^a Columbia University, New York, NY 10027

^b Institute for High Energy Physics, Peking, P.R. China

^c SLAC, Stanford, CA 94305

^d Sandia Laboratory, Albuquerque, NM 87185

^e Albert Ludwigs University, Freiburg, F.R. Germany

^f Hughes Aircraft Co., El Segundo, CA 90245

^g National Laboratory for High Energy Physics,
Tsukuba-gun, Ibaraki-ken 305, Japan

^h Fermi National Accelerator Laboratory, Batavia,
IL 60510

Abstract

The energy dependence of the cross section for neutrino and antineutrino-nucleon charged current interactions has been determined from data taken in Fermilab's dichromatic neutrino beam. We find $\sigma^{\nu}/E = 0.669 \pm 0.003 \pm 0.024 \times 10^{-38} \text{ cm}^2/\text{GeV}$ and $\sigma^{\bar{\nu}}/E = 0.340 \pm 0.003 \pm 0.02 \times 10^{-38} \text{ cm}^2/\text{GeV}$. These results are higher than some previous measurements.

Measurements of neutrino-nucleon scattering at high energies have been very important in verifying the constituent quark model of the nucleon. In this model, which incorporates approximate scaling,¹ the charged current cross sections for neutrinos and antineutrinos are predicted to rise almost linearly with beam energy; the slope of this rise (σ/E) is related directly to integrals of the structure functions at fixed neutrino energy. We report here measurements of high energy neutrino-nucleon cross sections which are higher than some previous measurements.²⁻⁶

Normalized neutrino cross sections are most accurately measured by using a dichromatic beam (i.e. from a momentum analyzed π , K beam) as the neutrino source. The precision tends to be limited by uncertainties in flux measuring and calibration and by the event statistics. The high statistics measurement presented here is based on a total event sample of 150,000 ν_{μ} events and 23,000 $\bar{\nu}_{\mu}$ events. The experiment was performed in the Fermilab neutrino area (E616) using the NO dichromatic beam⁷ and the Lab E iron detector.⁸⁻¹⁰ The flux was monitored by ion chambers that were calibrated using several independent methods.¹¹

The cross section in a specific energy range is given by the expression, $\sigma = N_{ev} / (F_{\nu} N_n)$, where N_{ev} is the number of charged current events occurring in some fiducial

volume of the detector, F_ν is the flux of incident muon neutrinos from the decay-in-flight of π and K mesons, and N_n is the number of target nucleons in this volume.

The flux (F_ν) is calculated from measurement of the number of pions and kaons and from their momentum and angular distributions. The beam of π 's, K's and protons was sign and momentum selected ($\Delta p/p = \pm 9.4\%$) before it traversed a 350 m long decay region. The relative populations of the particle types were measured with a focusing Cerenkov counter. Typical rms errors were 1% to 4% for pions and 4% to 7% for kaons.¹² The magnitude of the hadron flux was monitored by ion chambers at two separated locations along the decay region. The calibration¹² of these ion chambers is discussed in detail elsewhere.

The magnetic elements of the secondary beam line were energized under ten separate operating conditions to transmit and focus 120, 140, 168, 200, and 250 GeV/c positive or negative secondary hadrons. In the dichromatic beam, neutrinos from $K \rightarrow \mu \nu_\mu$ populate energies near the hadron beam energy and neutrinos from $\pi \rightarrow \mu \nu_\mu$ cover a range below 0.43 of the beam setting. Neutrino and anti-neutrino interaction events were collected over the energy range 30 to 250 GeV. The choice of settings permitted data with some overlap in neutrino energy from setting to setting. The cross sections from data in the overlapping energy ranges agree well.

The events (N_{ev}) were detected using the Lab E detector, 8-10 consisting of a 640 ton target region 3 m x 3 m in cross section, with full area calorimetry counters located every 10 cm of steel and spark chambers located every 20 cm of steel along the beam direction. Stringent fiducial cuts (e.g. the radius of interaction < 1.3 m from the center of the square target) and upstream veto requirements assure that all interactions occurred well within the iron target material. Cosmic ray events that survive these cuts comprise less than 0.5% of the sample as measured by recording data in the 10 sec intervals between the millisecond long beam bursts. The remaining subtracted background, due to neutrinos born upstream of the decay region, was measured in runs with the entrance to the decay region blocked.

Charged current interactions in the target contain a final state penetrating muon and hadrons that produce a shower in the iron calorimeter. This calorimeter was used to measure the hadron energy and a downstream toroidal magnet was used to measure the muon momentum. The calibrations and resolutions of these devices were obtained in a test beam of hadrons and muons of known energy. (The standard deviations were $\Delta E_h = 0.89 \sqrt{E_h}$ and $\Delta p_\mu = 0.11 p_\mu$ with energy in GeV.) Figure 1 shows the energy distribution for a typical data sample at the 250 GeV/c setting in a limited fiducial volume of the target. The dichromatic nature of the beam is evident and the identification of π and K decay neutrinos is unambiguous. 13

There were two separate triggers that responded to (a) the presence of a penetrating muon into the magnet downstream of the target ($E_{\mu} > 10$ GeV and polar lab angle $\theta_{\mu} < 100$ mrad); and (b) the presence of a minimum hadron energy deposition in the target ($E_h > 10$ GeV) and a penetrating muon ($E_{\mu} > 2.9$ GeV, $\theta_{\mu} < 370$ mrad). These triggers were formed from completely independent counters and logic circuitry. Typical events ($\sim 75\%$) were in a kinematic regime of trigger overlap allowing constant monitoring of trigger efficiencies. These were greater than 99% in all cases. Corrections, for losses from azimuthal inefficiencies for observing the muon, were calculated by a simple geometric rotation on an event-by-event basis. These corrections averaged less than 6% in magnitude. The measured events cover essentially all kinematic possibilities in this neutrino energy region, in an unbiased fashion,² for $\theta_{\mu} < 370$ mrad. Corrections for larger polar angles were made by calculations; they were generally small ($< 6\%$), decreasing to $< 1\%$ at higher energies. These corrections were insensitive to several different assumptions for the structure functions.¹⁴ As an example, the cross section would change by less than 1% at all energies if we were to use fits to our data¹⁵ as opposed to those published in Ref. 3.

The data presented here were taken during fast resonant extraction (~ 1 ms each machine cycle). The experiment could record only one event per machine cycle. The fraction of this beam to which the experiment was sensitive averaged 70% during neutrino running and 90%

during antineutrino running. This fraction was measured in two ways: by recording the flux during the triggerable and non-triggerable times, and by counting (but not recording) events during the non-triggerable time. The measurements of this fraction as obtained from the two methods typically agreed to 1%. Data were also taken during 1 sec long extraction of the beam during neutrino running. The experiment was sensitive for 85% of the flux for these data. The neutrino cross sections obtained with these data agreed to 1% with that from the fast resonant extraction data.

Table 1 shows our estimates of the largest contributions to the systematic errors quoted for individual ν_{μ} and $\bar{\nu}_{\mu}$ cross section values. Item (4) refers to possible misidentification of events as induced by π or K decay neutrinos due to improper event reconstruction. Item (5) refers to flux uncertainties due to the spread in neutrino angles, limited by our knowledge of the rms angular spread of the parent hadron beam, as measured by position sensing devices. The mean neutrino energy at a given target radius is determined in two ways: from the energy distribution of neutrino events and from the measurement of the mean momentum of the parent hadron beam. Item (6) was estimated from the agreement of the two techniques. In addition to the above errors, we have estimated an overall $\pm 3\%$ scale error on the ν_{μ} cross sections and $\pm 6\%$ on the $\bar{\nu}_{\mu}$ cross sections (not shown in Fig. 2). This error includes the ion chamber calibration error and the uncertainty in applying this calibration to the chamber and electronics used while taking data.

Figure 2 shows the neutrino and antineutrino cross sections divided by energy for the combined data. (These values also appear in Table 2.) The inner error bars are statistical; the outer include the systematic errors of Table 1. These cross sections contain small corrections (-2.1% for neutrinos, +1.4% for antineutrinos) to convert the iron target values to those of a pure isoscalar target. The data shown in Fig. 2 for both neutrinos and antineutrinos are consistent with being independent of energy. ($\chi^2/\text{degree of freedom} = 0.5$ for antineutrinos and 1.2 for neutrinos.)

The average slopes from this measurement are:

$$(\sigma/E)_{\nu} = (0.669 \pm 0.003 \pm 0.024) \times 10^{-38} \text{ cm}^2/\text{GeV}, \text{ and}$$

$$(\sigma/E)_{\bar{\nu}} = (0.340 \pm 0.003 \pm 0.020) \times 10^{-38} \text{ cm}^2/\text{GeV}.$$

The first error is statistical and the second systematic; the systematic error quoted includes the scale error mentioned above. The neutrino value agrees well with the cross section slope obtained using 200 GeV/c and 300 GeV/c beam settings during an engineering run preparatory to this experiment:⁹

$(0.70 \pm 0.04) \times 10^{-38} \text{ cm}^2/\text{GeV}$. However, these values are higher than some previously published results.²⁻⁶ Many of the participants in this measurement also participated in the earliest measurement,² which was lower.

The reasons for this difference are not fully understood.

Several aspects of the experimental technique have been considerably improved. The beam line, flux monitoring, calibrations, and neutrino detection apparatus are completely new, and are more sophisticated. Substantial

corrections to the flux monitor values and for lost events applied to the earliest result were not necessary for the result reported here.

In summary, we find normalized high energy neutrino and antineutrino cross sections to be higher than some earlier values. This result directly affects the fraction of momentum carried by struck quarks, as well as the normalization of quark model sum rules and structure functions.

We would like to acknowledge the Fermilab neutrino department and other departments at Fermilab for assistance during the preparation and execution of the experiment. This work was supported by the Department of Energy and the National Science Foundation.

References

- 1 R.P. Feynman, Phys. Rev. Lett. 23, 1415 (1969).
J.D. Bjorken, E.A. Paschos, Phys. Rev. 185, 1975 (1969).
- 2 B.C. Barish et al, Phys. Rev. Lett. 39, 1595 (1977).
 $\sigma_{\nu}/E = .609 \pm .030$ and $\sigma_{\bar{\nu}}/E = .290 \pm .015$.
- 3 J.G.H. deGroot et al, Z. Phys. C1, 143 (1979).
 $\sigma_{\nu}/E = .62 \pm .05$ and $\sigma_{\bar{\nu}}/E = .30 \pm .02$.
- 4 M. Jonker et al, Phys. Lett. 99B, 265 (1981). Errata 100B, 520;
103B, 469. $\sigma_{\nu}/E = .604 \pm .032$ and $\sigma_{\bar{\nu}}/E = .301 \pm .018$.
- 5 P. Bossetti et al, Phys. Lett. 110B, 167 (1982).
 $\sigma_{\nu}/E = .657 \pm .03$ and $\sigma_{\bar{\nu}}/E = .309 \pm .016$.
- 6 T. Kitagaki et al, Phys. Rev. Lett. 49, 98 (1982).
 $\sigma_{\nu}/E = .68 \pm .11$.
- 7 D.A. Edwards, F.J. Sciulli, "A Second Generation Narrow
Band Neutrino Beam", Fermilab TM-660 (1976).
- 8 B.C. Barish et al, IEEE Trans. on Nucl. Sci. NS-25,
532 (1978).
- 9 J. Lee, "Measurements of $\nu_{\mu}N$ Charged Current Cross Sections
from $E_{\nu} = 25$ GeV to $E_{\nu} = 260$ GeV", Ph.D. Thesis (1980),
Caltech, Pasadena, CA.
- 10 R. Blair, "A Total Cross Section and Y Distribution
Measurement for Muon Type Neutrinos and Antineutrinos",
Ph.D. Thesis (1982), Caltech, Pasadena, CA.
- 11 The flux measurement, and background measurements (such as
neutrinos from upstream sources), were provided to the two
bubble chamber groups (Hawaii-Berkeley-Fermilab and BNL-
Columbia-Rutgers) who accumulated data during part of the
same running period.

- 12 R. Blair et al, "A Monitoring and Calibration System for Neutrino Flux Measurement in a High Energy Dichromatic Neutrino Beam", Nevis Preprint 1983, Fermilab-Pub-83/26-Exp. To be submitted to Nucl. Instr. & Methods.
- 13 For a detailed description of the method used to separate π and K decay neutrino events, see Refs. 2, 9, and 10.
- 14 H.E. Fisk, F. Sciulli, Ann. Rev. Nucl. & Part. Sci. 32, 499 (1982).
- 15 R.E. Blair et al, "Neutrino Charged Current Structure Functions"; University of Rochester preprint (1982), UR-831.

Table 1: Approximate point-to-point errors in cross sections and their sources. Actual errors depend on energy setting and the position in the target.

	$\frac{\nu_{\pi}(\bar{\nu}_{\pi})}{\dots}$	$\frac{\nu_K(\bar{\nu}_K)}{\dots}$
1. Statistical counting errors, including empirically subtracted backgrounds	3%	8%
2. Particle fractions ($\pi/K/P$)	(1-4)%	(4-7)%
3. Monitoring stability and calibration	(2-5)%	(2-5)%
4. Crossover of events $\nu_{\pi} \leftrightarrow \nu_K$	0.7%	2.5%
5. Beam angular divergence errors	3%	2%
6. Neutrino energy error	1.5%	1.5%
7. Deadtime uncertainty	1%	1%

Neutrinos

E_ν (in GeV)	$\frac{\sigma^{\nu}}{E}$ (in $\frac{10^{-38} \text{cm}^2}{\text{GeV}}$) †
37.1	.654 ± .012 ± .019
44.7	.621 ± .010 ± .020
54.0	.661 ± .008 ± .018
63.5	.664 ± .010 ± .024
75.4	.664 ± .008 ± .028
91.0	.644 ± .015 ± .057
111.7	.659 ± .029 ± .058
124.8	.665 ± .020 ± .037
141.2	.695 ± .026 ± .043
157.4	.680 ± .018 ± .033
165.1	.714 ± .020 ± .035
179.8	.727 ± .015 ± .036
190.8	.749 ± .015 ± .035
212.5	.709 ± .014 ± .048
229.1	.756 ± .018 ± .052

Antineutrinos

E_ν (in GeV)	$\frac{\sigma^{\bar{\nu}}}{E}$ (in $\frac{10^{-38} \text{cm}^2}{\text{GeV}}$) ‡
36.9	.361 ± .010 ± .015
45.0	.352 ± .007 ± .013
54.0	.350 ± .007 ± .013
63.8	.332 ± .009 ± .014
75.6	.331 ± .009 ± .020
89.3	.333 ± .015 ± .031
110.3	.314 ± .022 ± .034
126.5	.341 ± .017 ± .032
150.0	.339 ± .015 ± .022
174.4	.321 ± .015 ± .021
201.9	.303 ± .017 ± .026

†(Errors are statistical first, systematic second,
and do not include an overall scale error of 8.%)

‡(Errors are as above, but the overall scale error is 5.5%)

TABLE II: Neutrino and antineutrino cross section slopes.

Figure Captions

Fig. 1 Solid histogram: Distribution in observed total energy for events inside a single radial bin of interaction points at the target ($25.4 \text{ cm} < R < 50.8 \text{ cm}$) for the +250 GeV/c fast spill data. This separation is typical of data at all radii and beam settings. (Note the logarithmic scale.)

Dashed histogram: Observed energy distribution for events obtained when the entrance to the decay region is blocked (wide-band background). These data have been normalized to the same number of incident protons as the data in the solid curve.

Smooth curve: Calculated ν_{μ} events from $K_{\mu 3}$ decay neutrinos, normalized to the events in the ν_K peak.

Fig. 2 Cross section slope for neutrinos and anti-neutrinos versus energy for the data from this experiment. The values in this plot are available in Ref. 15.

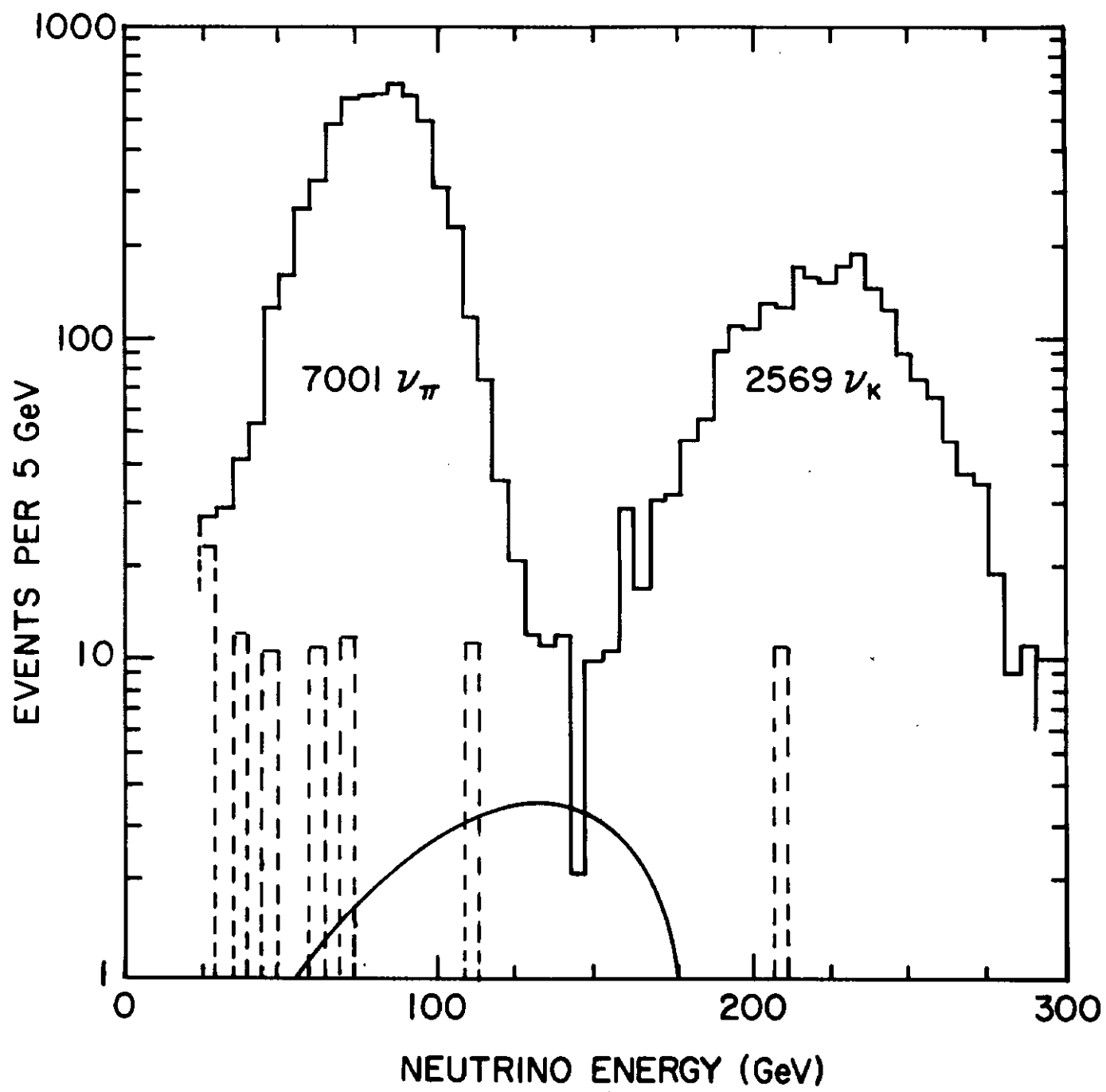


Figure 1

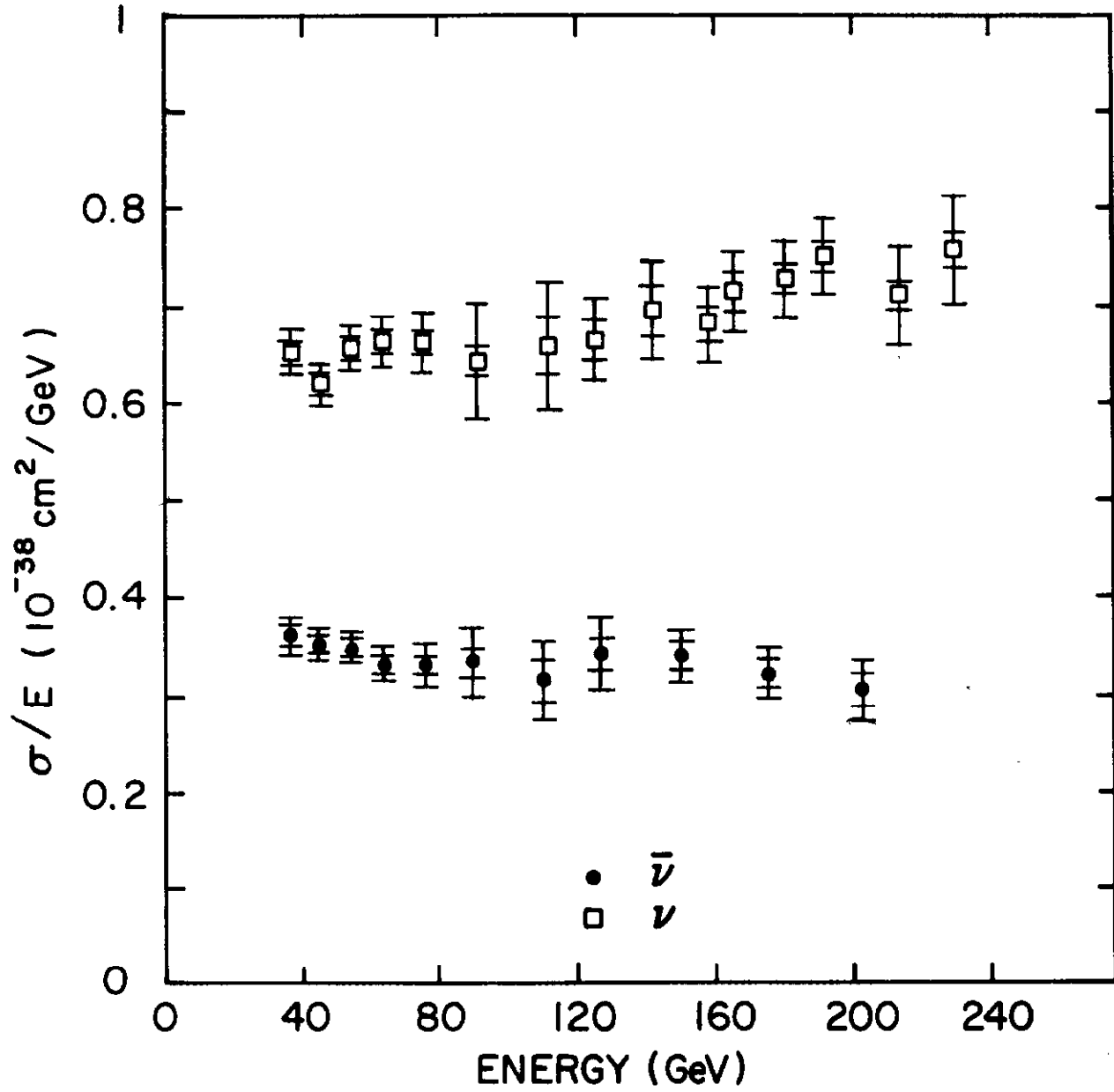


Figure 2